Effects of Fuel Distribution on Detonation Tube Performance

H. Douglas Perkins[*]

NASA Glenn Research Center, Cleveland, Ohio 44135

and

Chih-Jen Sung[**]

Department of Mechanical and Aerospace Engineering
Case Western Reserve University, Cleveland, Ohio 44106

Abstract

A pulse detonation engine uses a series of high frequency intermittent detonation tubes to generate thrust. The process of filling the detonation tube with fuel and air for each cycle may yield non-uniform mixtures. Uniform mixing is commonly assumed when calculating detonation tube thrust performance. In this study, detonation cycles featuring idealized non-uniform H_2/air mixtures were analyzed using a two-dimensional Navier-Stokes computational fluid dynamics code with detailed chemistry. Mixture non-uniformities examined included axial equivalence ratio gradients, transverse equivalence ratio gradients, and partially fueled tubes. Three different average test section equivalence ratios were studied; one stoichiometric, one fuel lean, and one fuel rich. All mixtures were detonable throughout the detonation tube. Various mixtures representing the same average test section equivalence ratio were shown to have specific impulses within 1% of each other, indicating that good fuel/air mixing is not a prerequisite for optimal detonation tube performance under the conditions investigated.

[*] Aerospace Engineer, Hypersonics Projects Office, Hugh.D.Perkins@grc.nasa.gov. Member AIAA.
[**] Associate Professor, Department of Mechanical and Aerospace Engineering, cjs15@po.cwru.edu. Senior Member AIAA.

Introduction

The concept of a pulse detonation engine (PDE) for aerospace propulsion system applications is not new. The work at the University of Michigan in the 1950's is a prime example[1]. However, it was not until repetitive detonations with gaseous hydrocarbon fuels at relatively high frequencies were demonstrated in the mid-1980's that it became apparent that practical devices might be possible. These advances and others over the past decade have stimulated interest in the mainstream propulsion development community[2,3]. Government and industry organizations are currently developing PDE's and derivative configurations for missions as diverse as missiles, tactical aircraft, commercial aircraft, and launch vehicles[4]. At the heart of each of these unique propulsion systems is a series of high frequency intermittent (pulse) detonation tubes.

PDE's are attractive for several reasons. First, Kailasanath and Patniak[5], among others, have shown that the thermal efficiency of the detonation cycle can be significantly higher than the thermal efficiency of the standard Brayton cycle found in gas turbine engines and ramjets, 49% versus 27% in an example case where both combustion processes begin at 1 atmosphere pressure. Second, since static pressure increases significantly during detonative combustion, instead of decreasing slightly as in deflagrative combustion, it is possible to decrease the amount of compression required before the combustion process, thus leading to simplified, lighter, lower cost engine architectures. For some missions, such as air-launched missiles, it is possible to eliminate all mechanical pre-compression and operate the PDE as a "supercharged" ramjet, even at relatively low subsonic Mach numbers. Lastly, a PDE detonation chamber does not have to be round, nor do the detonation chambers have to be grouped in circular arrays if turbomachinery

components have been eliminated, thus leading to a more aerodynamically efficient airframe integration than with a gas turbine engine.

It is likely that in any application of detonative combustion for propulsion, the fuel and air will not be uniformly mixed, as is typically assumed. Non-uniformity in fuel distribution may be created intentionally or may result from hardware limitations, and may be either axial or transverse, or both, depending on the source. Possible sources of non-uniform fuel distribution include, but are not limited to,

- Combustion products/fresh charge buffering (purge)

- Engine throttling

- Emissions control

- Wall heat transfer control

- Detonation wave shape/strength control

- Air and fuel valve transients

- Non-uniform inlet air flow in space and time.

The study that follows examines the effects of various idealized fuel distribution non-uniformities on detonation tube thrust performance (specific impulse, I_{sp}). Kailasanath et al.[6] studied the performance effects of unfueled volumetric purge fraction, alternately referred to as partial fill, showing an increase in I_{sp} with increasing purge fraction (decreasing fill fraction). This study was conducted using a transversely uniform stoichiometric mixture of ethylene and air in the fueled portion of the tube, leaving the exit end of the tube unfueled. No spatial transition (gradient) in equivalence ratio was used between the two regions. Purge fractions of up to 80% were studied. Note that this approach simultaneously changed the fuel distribution within the tube and the overall equivalence ratio. The current study builds upon and expands the

3

consideration of fuel distribution effects by looking at the effects of various axial equivalence ratio gradients, transverse equivalence ratio gradients, and partial fills while maintaining constant overall equivalence ratios. The numerical results are intended to be comparative in nature, looking for trends and relative magnitude effects between the different cases. The actual values of performance are not validated by test data, and so may be subject to some level of offset error. However, it is expected that the physics-based numerical modeling techniques employed will provide correct insight into the relative performance effects of the different fuel distributions.

Problem Formulation

Computation Domain

The geometry of a detonation tube is generally simple outside of the detonation initiation section upstream of the main detonation chamber. While the geometry of the detonation initiation section is critical to the operability of the device, this study is confined to the constant-area main detonation chamber. This region represents the majority of the volumetric capacity and therefore energy release within the device, making it the dominant region in terms of thrust performance. To keep the geometry as simple as possible, the inflow plane (main air inlet valves) will be modeled as a solid wall, simulating a transitioned detonation with the inlet valves closed.

Typical proof-of-concept PDE detonation tubes being used today are on the order of 5 to 15 cm in diameter and 100 to 300 cm in overall length (including the detonation initiation section). For this study a height of 3.0 cm and a length of 30.0 cm will be used in order to limit the computational time required. This basic two-dimensional geometry is shown in Figure 1.
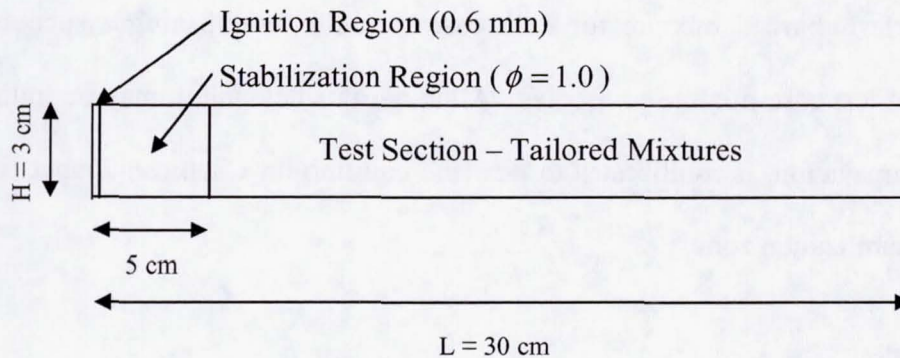
Figure 1 – Geometry for Numerical Study

Assumptions

A number of simplifying assumptions are made in this study relative to the actual PDE cycle, as follows.

Deflagration to Detonation Transition:

No attempt is made to model the deflagration to detonation transition (DDT) process, as the phenomena under study are primarily concerned with the steady state detonation propagation. As shown in Figure 1, the initiator tube itself is not modeled nor is any area change from the initiator to the main chamber modeled. A successfully transitioned detonation wave is numerically initiated through the imposition of a high temperature, high pressure ignition zone at the left-hand (inflow) side of the domain in a 5.0 cm initiation/stabilization region. The high pressure, high temperature ignition zone is set uniformly to 150 atmospheres, 4000 K, and is the full height of the tube, but only 0.6 mm long, with a composition of 25.5% H_2O and 74.5% N_2 by weight. The total energy contained in the ignition region is 335 J, which is approximately 1.3% of the heat release from the full 30 cm detonation tube when it is uniformly, stoichiometrically

5

fueled (26.2 KJ). The remaining 4.94 cm stabilization region is maintained as a uniform, stoichiometric unburned mixture for each case to aid in establishing a successful detonation regardless of test case mixture properties. Although this detonation may be initially overdriven to insure propagation, it equilibrates to near the equilibrium Chapman-Jouget condition by the end of the stabilization zone.

Partial Cycle:

Only the detonation propagation and blowdown portions of the full PDE cycle are modeled. It is assumed that the purge and refresh cycles are identical for each case. While this might not be rigorously true in practice, such differences would be expected to be of significantly less importance. It is further assumed that the blowdown of the tube is complete when the tube exit velocity reaches zero anywhere along the exit plane. In a real cycle, some backflow is likely to occur due to the sub-ambient pressure in the tube from the last reflected expansion wave. This portion of the cycle is important when modeling the filling of the tube, both in terms of the fill time and the performance penalty, but this issue is beyond the scope of this study.

Fuel-Air Combinations

A stoichiometrically fueled 5.0 cm detonation initiation section is used to provide a stabilized detonation wave to the test section. The test section equivalence ratio is varied in either the X-direction (axial) or the Y-direction (transverse) from case to case. Three test section average equivalence ratios, alternately denoted as Φ or "Phi", are used, one stoichiometric, one fuel-lean, and one fuel rich. Non-stoichiometric equivalence ratios of 0.9 and 1.1 were selected, representative of moderate levels of non-uniformity, but still well within expected stable detonation limits throughout the detonation tube. Different buffers or gradients of fuel/air

mixture are used to achieve the desired average test section equivalence ratio. Transverse gradient cases are representative of a tube centerline fuel injection configuration, while axial gradient cases are representative of a non-constant tube filling process brought on by time varying tube inlet and exit conditions. Partial fill cases are representative of fuel lead (H_2 buffer) or fuel lag (air buffer) injection timing. Baseline uniformly fueled cases are used to normalize the results of the subsequent cases. The test cases are grouped as follows, with Φ referencing the test section average equivalence ratio and ϕ referencing the local equivalence ratio within the test section.

Stoichiometric Combustion ($\Phi = 1.00$)

Case 1 – Baseline – uniformly fueled throughout test section.

Case 2 – Linear transverse gradient - $\phi = 1.10$ at the centerline; $\phi = 0.90$ at each wall.

Case 3 – Linear axial gradient - $\phi = 1.10$ at the closed end (after the initial stabilization zone); $\phi = 0.90$ at the open end.

Case 4 – Linear transverse gradient - $\phi = 1.20$ at the centerline; $\phi = 0.80$ at each wall.

Case 5 – Linear axial gradient - $\phi = 1.20$ at the closed end (after the initial stabilization zone); $\phi = 0.80$ at the open end.

<u>Fuel-Lean Combustion</u> ($\Phi = 0.90$)

Case 6 – Baseline – uniformly fueled throughout test section.

Case 7 – Linear transverse gradient - $\phi = 1.00$ at the centerline; $\phi = 0.80$ at each wall.

Case 8 – Linear axial gradient - $\phi = 1.00$ at the closed end (after the initial stabilization zone); $\phi = 0.80$ at the open end.

Case 9 – 2.50 cm air buffer at the end of the test section; $\phi = 1.00$ up to the buffer air in the test section.

<u>Fuel-Rich Combustion</u> ($\Phi = 1.10$)

Case 10 – Baseline – uniformly fueled throughout test section.

Case 11 – Linear transverse gradient - $\phi = 1.20$ at the centerline; $\phi = 1.00$ at each wall.

Case 12 – Linear axial gradient - $\phi = 1.20$ at the closed end (after the initial stabilization zone); $\phi = 1.00$ at the open end.

Case 13 – 0.07 cm H_2 buffer at the end of the test section; $\phi = 1.00$ up to the buffer H_2.

Figures 2 and 3 show graphically the different axial and transverse fuel distribution schemes to be used in the "test section" of the detonation tube, excluding the baseline uniformly fueled cases (Cases 1, 6, and 10) and the partial-fill cases (Cases 9 and 13).
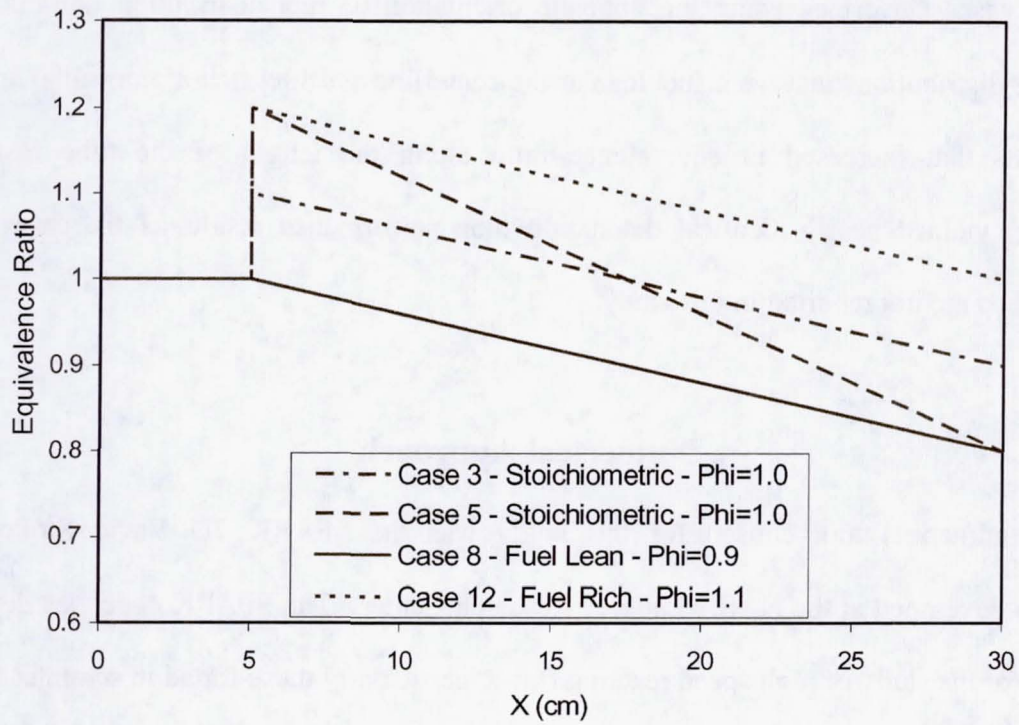
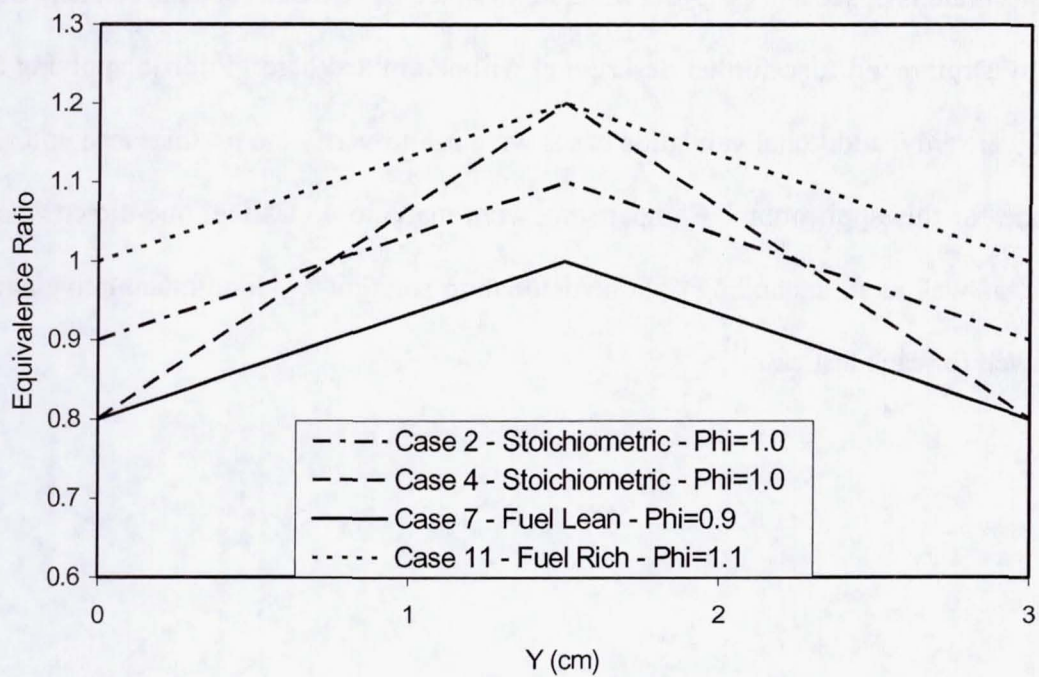Figure 2 – Test Section Axial Fuel Distributions

Figure 3 – Test Section Transverse Fuel Distributions

Test cases performed using the opposite orientation of fuel distribution non-uniformity (transverse distributions that were fuel lean at the centerline and fuel rich at the walls, and axial distributions that increased in equivalence ratio along the length of the tube instead of decreasing) yielded nearly identical detonation tube performance results as the cases shown above, and so are not reported in this study.

Numerical Approach

The numerical tool chosen for this study was the SPARK 2D Navier-Stokes Code previously developed at the NASA Langley Research Center. The SPARK code was developed primarily for the study of high speed reacting flows, particularly those found in scramjet engines, and has been used in a number of supersonic combustion and detonation studies[7-9]. The governing equations are solved using a MacCormack explicit predictor-corrector scheme that is 4th order accurate in space and 2nd order accurate in time. SPARK has been previously described in detail by Drummond[10], so further description will be omitted here. Prior to applying SPARK to the subject study, additional validation cases were run to verify the performance and accuracy of the code for this application. Comparisons were made to a classical one-dimensional ZND solution[11], as well as to a standing oblique detonation solution[12]. Good quantitative agreement was achieved for each test case[13].

Detailed Chemistry

Following the work of Cambier and Adelman[14] and Lynch and Edelman[15], a 7-step, 7-species hydrogen-air detailed chemical mechanism was chosen for this study instead of the more standard 18-step, 9-species mechanism of Jachimowski[16]. For computational efficiency, it is desirable to utilize the simplest possible mechanism that can with reasonable accuracy provide the correct time evolution and chemical composition of the detonation wave and the resultant combustion products. The 7-step mechanism is a simple reduction of the 18-step mechanism through the elimination of HO_2 and H_2O_2 from the chemical system, leaving H_2, O_2, H_2O, OH, H, O, and N_2 (inert). This simplification can be justified when it is considered that in the basic ZND detonation model, ignition occurs after the leading shock, at which point the flow temperature is elevated to a point where the chemistry of HO_2 and H_2O_2 is no longer important.

Thermodynamic and Transport Properties

SPARK utilizes previously developed analytical expressions for the required thermodynamic and transport properties used throughout the code, which, as with the previously discussed aspects of the code, have been related in detail in other publications, such as Drummond[10]. Species specific heat at constant pressure and species Gibbs energy are calculated using 4th and 5th order polynomial curve fits of temperature, respectively. The species laminar viscosity and mixture viscosity are calculated using analytical expressions commonly referred to as Sutherland's law and Wilke's law. Lastly, the binary diffusion coefficient and the thermal conductivity are calculated from the Schmidt number and Prandtl number, respectively, which are provided as inputs to the code. All properties were calculated assuming laminar flow throughout.

Computational Grid

It is readily apparent that the region in the immediate vicinity of the detonation wave front will determine the required physical grid spacing for the computational model. If the goal of this study were to examine the detailed structure of the shock wave coupled to the reaction zone, it would be necessary to provide a computational grid spacing on the order of the width of the leading shock wave (on the order of 1.4×10^{-7} m)[17], and probably finer. Fortunately, it is not necessary to resolve this structure in order to accurately obtain flow properties required to calculate the performance values that are the goal of this study. It is sufficient to provide enough grid resolution to capture the shortest reaction times of the chemical system as the flow behind the shock is convected downstream. For the 7-step chemical system and conditions investigated in this study, this worked out to be on the order of 1×10^{-5} m. Since an X-grid spacing of 1×10^{-5} m would yield 30,000 grid points in the X-direction for each Y-grid location for a 30 cm tube, it becomes immediately apparent that this grid spacing needs to be confined to the region where it is required, namely the leading section of the detonation wave where steep gradients in all the principal flow and composition variables are present. Since the detonation wave is moving in space, the fine grid must move with it. This was accomplished for this study by starting with a uniform 300-point grid in X at the fine grid spacing (1×10^{-5} m). As the detonation wave approaches the right-hand edge of the computational domain, the grid is stretched by approximately 30 times the fine grid spacing at the left hand side where the reaction has already occurred, lengthening the overall domain in X. The wave structure is thus always maintained within the fine grid section, which is effectively shifted to the right every time the detonation wave travels 30 times the fine grid spacing. The current result is then interpolated onto the new

grid and the calculation is continued. Once the desired length of the full detonation tube is reached, the fine grid is maintained at the right hand (exit) end of the tube.

The Y-grid spacing remains the same throughout each calculation. 100 grid points were used in the Y direction, with finer grid spacing used near the wall in order to capture with reasonable fidelity the severe gradient of velocity generated by the detonation wave in that region. The maximum Y-grid spacing was 1×10^{-3} m at the tube centerline. As with the X-grid, significantly finer grid spacing yields proportionally smaller time steps, leading to excessively long computational times. Grid spacing as small as 5×10^{-6} m at the wall did not require time steps smaller than those required for the finite-rate chemistry. Minor adjustments to the Y-grid spacing were used case-to-case to minimize run times while maintaining detonation wave stability.

Boundary Conditions

The left-hand, top and bottom walls of the two-dimensional detonation tube are all treated as impermeable, dictating that the pressure derivative, the species concentration derivatives, and the normal component of velocity be set to zero at each wall. No-slip and adiabatic conditions are set at each surface by setting the parallel component of velocity and the temperature derivative to zero.

The tube exit boundary conditions for this type of calculation have been a source of considerable study, with various approaches having been used by different individuals, such as Kailasanath and Patnaik[5], and Wilson and Paxson[18]. The approach of Wilson and Paxson[18] for long detonation tubes (L/H>7) was followed in this study, wherein the supersonic and choked flow conditions present during the first part of the tube blowdown preclude any effect from the

13

decaying blast wave outside the tube on the tube internal flow. Once the tube pressure has dropped sufficiently for the exit to be un-choked, the blast wave is far enough away from the exit so as to be of no further concern. The supersonic and choked flow boundary conditions were extrapolated from interior grid points, while the methodology of Poinsot and Lele[19] was used for the characteristic subsonic reflecting outflow boundary condition. Each exit grid point was checked at each time step to determine which boundary condition was required.

Computational Results

Before examining the detonation tube performance results, it is of value to look at some typical results in detail to establish the accuracy and stability of the calculations, as well as the general character of the flowfield generated by the detonation process. Figure 4 shows the tube centerline detonation wave speeds for Cases 1 through 3, the first three overall stoichiometric cases. These wave speeds can be compared to the equilibrium Chapman-Jouget wave speeds of 1923 m/s for $\phi = 0.90$, 1969 m/s for $\phi = 1.00$, and 2005 m/s for $\phi = 1.10$, as calculated using the NASA Glenn CEA code[20]. The initial overshoot results from the high pressure, high temperature detonation initiation process that is overdriven to insure a well established detonation in the test section. The change in detonation wave speed at approximately 2.0×10^{-5} seconds is caused by the wave exiting the uniformly fueled detonation stabilization zone and entering the test mixture. Case 1, the uniform mixture case, asymptotically approaches the $\phi = 1.00$ Chapman-Jouget wave speed, achieving a wave speed of 1953 m/s before exiting the detonation tube. Case 2, the transversely varying mixture, initially responds to the higher equivalence ratio along the tube centerline upon entering the test section before settling back to follow the same wave speed characteristic as Case 1. Case 3, the axially varying mixture,

accelerates upward toward the $\phi = 1.10$ Chapman-Jouget wave speed as the wave enters the test section, then falls off linearly in direct correlation to the change in test section equivalence ratio. The Case 3 wave speed always stays just below the equilibrium wave speed, exiting the tube at a speed of 1903 m/s. In all cases, final wave speeds within 3% of the equilibrium value were achieved.
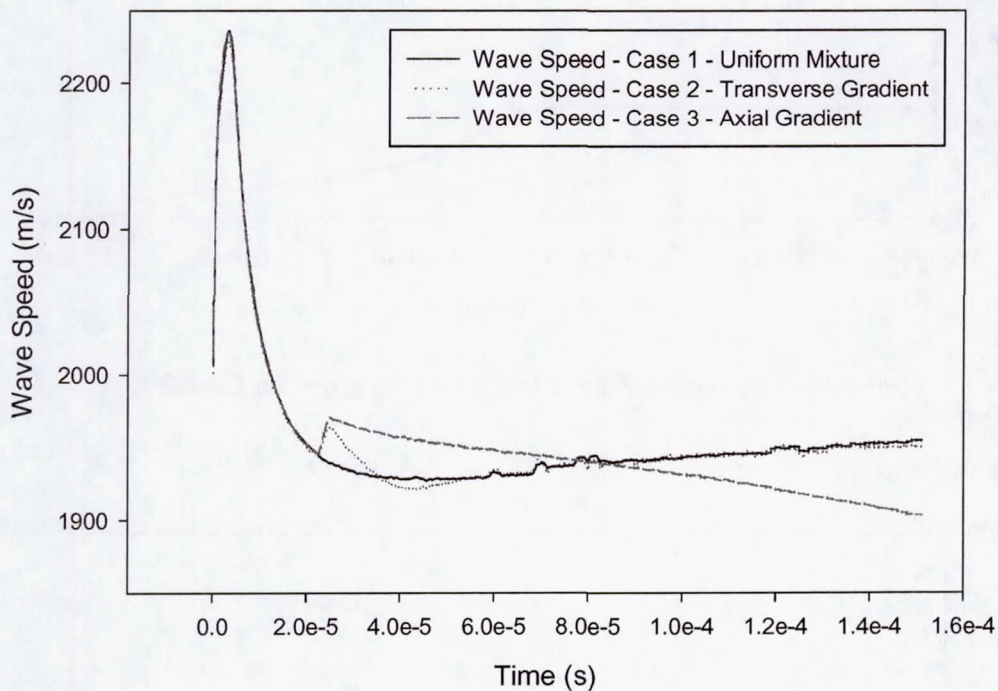

Figure 4 – Detonation Wave Speeds for Stoichiometric Cases 1, 2, and 3

Figures 5 and 6 show the detonation tube closed-end pressure and resulting specific impulse as functions of time for Case 2. These plots show a well-behaved tube blowdown process consistent with previous published results[5], and are typical of all the cases studied.
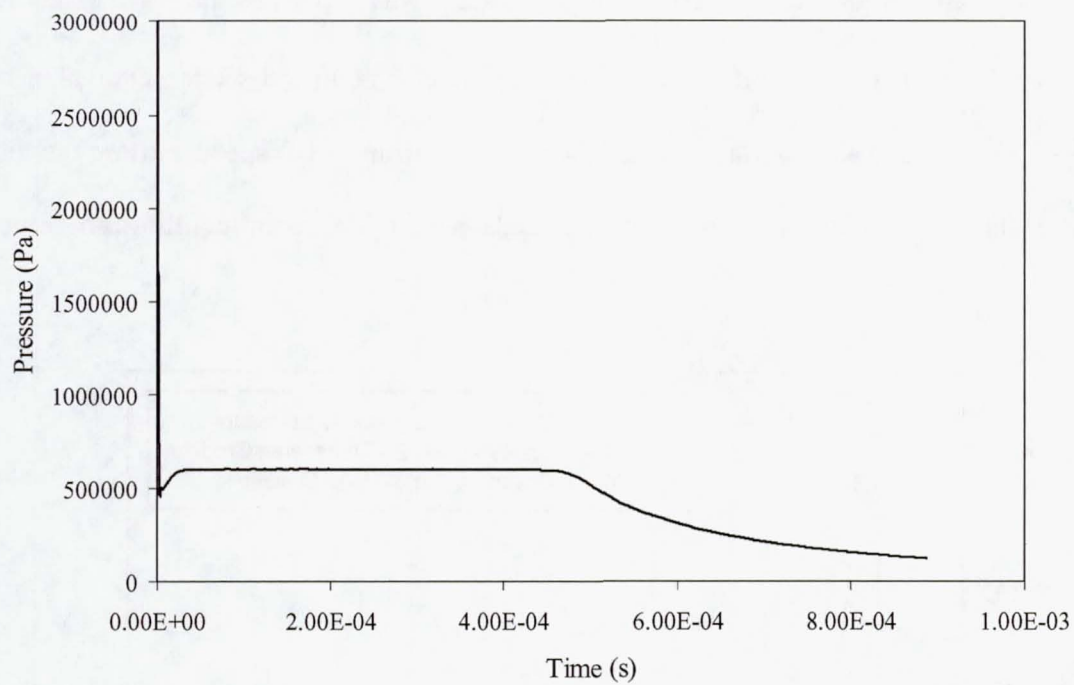
15

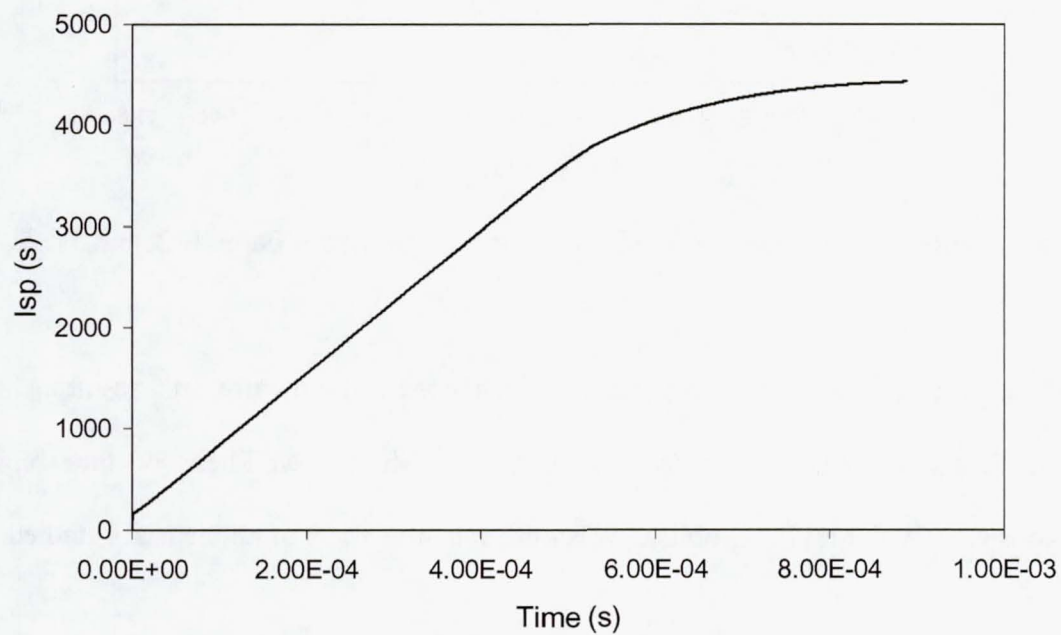Figure 5 – Detonation Tube Closed End Pressure for Case 2

Figure 6 – I_{sp} Time History for Case 2

Furthermore, we can look at plots of H_2 mass fraction to determine if any significant flow irregularities are occurring during either the detonation wave propagation or tube blowdown. Figure 7 shows the hydrogen mass fraction in the tube at five different times for Case 2, which would be expected to show the greatest two-dimensional behavior due to the transverse mixture variation. The first three plots are during the detonation propagation, and the last two plots are during the blowdown. The post-detonation H_2 distribution remains essentially stratified throughout the entire propagation and blowdown, with the composition distribution at the left of the tube stretching to the right to fill the tube as the blowdown progresses. The products of the uniformly fueled stoichiometric stabilization zone eventually push out most of the stratified combustion products by the end of the simulation. The relatively high levels of residual H_2 at the left-hand (closed) end of the tube seen in this time sequence are a result of the thermal breakdown of H_2O in the high pressure, high temperature region used to initiate the detonation and are not a product of the detonation process itself. These results are again typical of all of the test cases run in this study, both for transversely and axially varying mixtures.
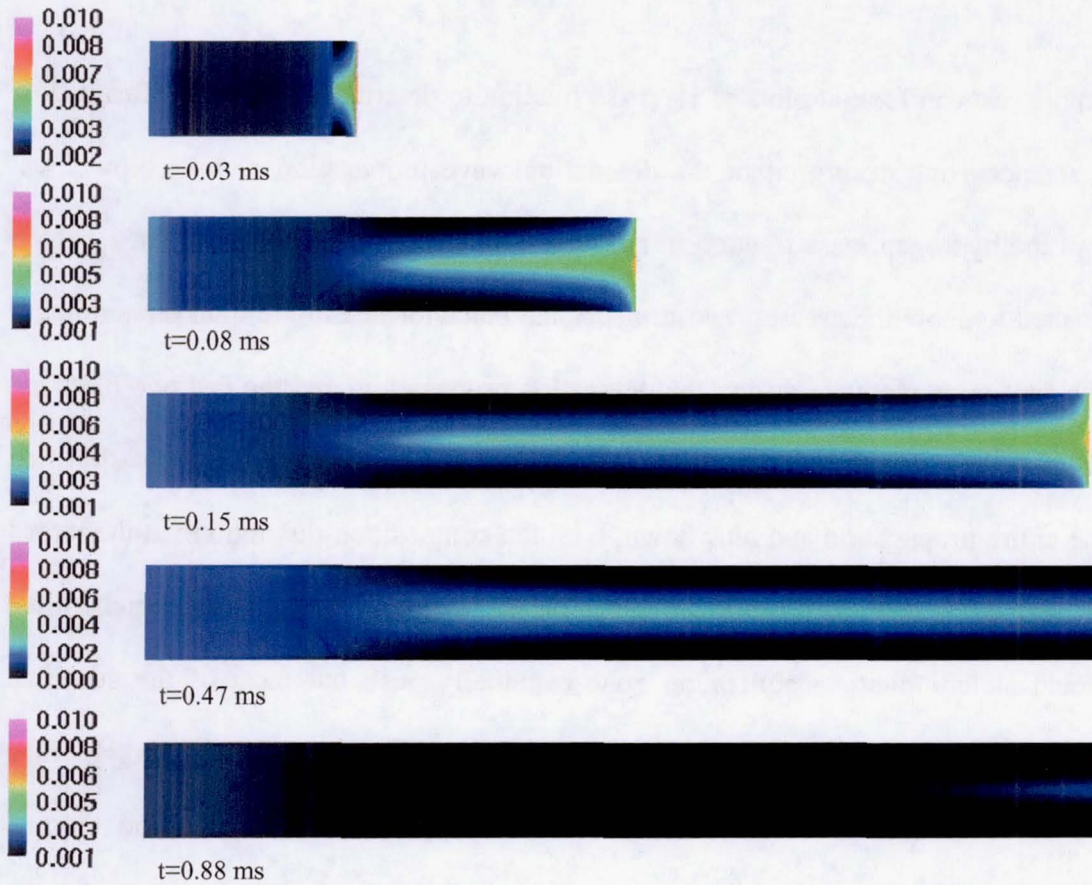
Figure 7 – Two-Dimensional H_2 Mass Fraction Distributions for Case 2 –

Transverse Gradient

Moving on to the performance results, Table 1 below summarizes the final specific impulse results of the 13 cases run in this study. Several comparisons can be made to illuminate the effects of mixing and equivalence ratio.

1. Comparing the cases within each equivalence ratio grouping, it is readily seen that the case-to-case variation in specific impulse is less than 1%. While there is some trending within the results, transverse mixtures performing slightly worse in all cases, for instance, the level of variation in performance should be considered negligible.

2. Comparing the uniform mixture baseline Cases 6 and 10 with the corresponding partial fill Cases 9 and 13, it is seen that there is no particular advantage of partial fill over a uniform mixture with the same overall stoichiometry.

3. By plotting the results for the uniformly fueled baseline Cases 1, 6, and 10, as shown in Figure 8, it is seen that I_{sp} is essentially linear with equivalence ratio in the limited range of equivalence ratios studied herein. Inclusion of the stabilization zone raises the overall equivalence ratio of the fuel lean cases to 0.92, and lowers the overall equivalence ratio of the fuel rich cases to 1.08. Since the effect of the stabilization zone cannot be isolated within the calculation, this equivalence ratio bias is included in all I_{sp} calculations.

Case Number	Overall Stoichiometry	Type of Distribution	Final I_{sp} (s)
1	Stoichiometric	Uniform	4450
2	Stoichiometric	Transverse $\phi = 0.9$ to 1.1	4429
3	Stoichiometric	Axial $\phi = 0.9$ to 1.1	4459
4	Stoichiometric	Transverse $\phi = 0.8$ to 1.2	4410
5	Stoichiometric	Axial $\phi = 0.8$ to 1.2	4440
6	Fuel Lean	Uniform	4706
7	Fuel Lean	Transverse	4699
8	Fuel Lean	Axial	4722
9	Fuel Lean	Partial Fill (Air)	4676
10	Fuel Rich	Uniform	4177
11	Fuel Rich	Transverse	4168
12	Fuel Rich	Axial	4175
13	Fuel Rich	Partial Fill (H_2)	4204

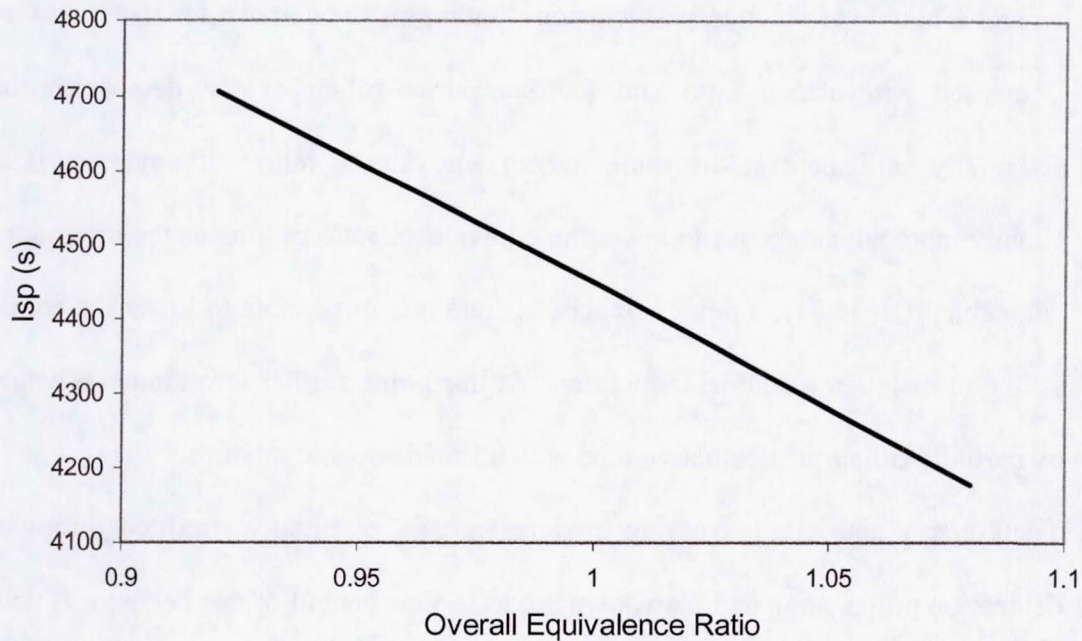Table 1 – Summary of Test Case Performance Results

Figure 8 – Final I_{sp} as a Function of Overall Equivalence Ratio, including Stabilization Zone, for

Cases 1, 6, and 10

Conclusions

The primary conclusion to be drawn from this study is that a lack of fuel-air mixing up to a moderate level in a hydrogen fueled air-breathing detonation tube has almost no effect on the thrust performance of the system. Put another way, thrust performance is almost completely independent of combustion efficiency in the vicinity of an overall equivalence ratio of one. This is an encouraging result for the design of such systems, as it appears to be unnecessary to go to extremes to achieve good mixing in the fuel injection process. These results also imply that it is probably unnecessary to precisely match air and fuel valve opening and closing profiles to maintain constant equivalence ratio. These results are limited to those cases where the entire fuel/air charge, while not fully mixed, is nonetheless fully detonable.

21

There are a couple of secondary conclusions that may also be drawn for H_2/air systems.

1. Decreased equivalence ratio and fuel-lag partial-filling of the detonation tube are essentially equivalent at the same overall equivalence ratio. If anything, it appears slightly more advantageous to lower the equivalence ratio as long as the mixture remains detonable. Obviously, a point is reached where it is impossible to lower the equivalence ratio and maintain a detonable mixture. At this point, further throttling can be achieved by partially filling the detonation tube with a lean detonable mixture.

2. Transversely and axially varying mixtures remain essentially stratified throughout the detonation propagation and blowdown process. One benefit of this behavior is that it will be possible to qualitatively evaluate mixing within a detonation tube by looking at the temporal and spatial distribution of products coming out of the tube, thus reducing the need for costly optical test sections in detonation tubes. A related conclusion is that one-dimensional simulations are adequate for non-transversely varying mixtures. Since there was minimal mixing or shear effect observed, despite the no-slip condition maintained at the wall, a one-dimensional simulation should capture the principal effects of the detonation propagation and blowdown.

Acknowledgements

References

[1]Nichols, J., Wilkinson, H., and Morrison, R., "Intermittent Detonation as a Thrust Producing Mechanism," Jet Propulsion Journal of the American Rocket Society, Vol. 27, No. 5, 1957, pp. 534-541.

[2]Kailasanath, K., "Applications of Detonations to Propulsion: A Review," AIAA Paper 99-1067, January 1999.

[3]Kaemming, T.A., "Integrated Vehicle Comparison of Turbo-Ramjet Engine and Pulsed Detonation Engine (PDE)," ASME Paper 2001-GT-0451, June 2001.

[4]Coleman, M.L., "Overview of Pulse Detonation Propulsion Technology," CPIA Report No. CPTR 70, April 2001.

[5]Kailasanath, K., and Patnaik, G., "Pulsed Detonation Engines – What is its Performance," Proceedings of the 24th JANNAF Airbreathing Propulsion Subcommittee and 36th JANNAF Combustion Subcommittee Joint Meeting, CPIA Publication 692, Vol. 1, October 1999, pp. 131-140.

[6]Kailasanath, K., Patnaik, G., and Li, C., "On Factors Controlling the Performance of Pulsed Detonation Engines," in *Control of Detonation Processes,* G. Roy et al. editors. Elex-KM, Moscow, 2000, pp. 172-174.

[7]Drummond J.P., and Mukunda, H.S., "A Numerical Study of Mixing Enhancement in Supersonic Reacting Flow Fields," AIAA Paper 88-3260, July 1988.

[8]Drummond, J.P., "A Two-Dimensional Numerical Simulation of a Supersonic, Chemically Reacting Mixing Layer," NASA TM-4055, 1988.

[9]Carpenter, M.H., "Three-Dimensional Computations of Cross-Flow Injection and Combustion in a Supersonic Flow," AIAA 89-1870, June 1989.

[10]Drummond, J.P., "Supersonic Reacting Internal Flow Fields," NASA TM-103480, 1990.

[11]Shepherd, J.E., "Chemical Kinetics of Hydrogen-Air-Diluent Detonation," Dynamics of Explosions, edited by Bowen, J.R., Vol. 106, *Progress in Astronautics and Aeronautics*, AIAA, New York, 1986, pp. 263-293.

[12]Thaker A.A., and Chelliah, H.K., "Numerical Prediction of Oblique Detonation Wave Structures Using Detailed and Reduced Reaction Mechanisms," Combustion Theory Modelling, Vol. 1, 1997, pp. 347-376.

[13]Perkins, H.D., "Effects of Fuel Distribution on Detonation Tube Performance," M. S. Thesis, Case Western Reserve University, 2002. (also NASA TM-2002-211712)

[14]Cambier, J.-L., and Adelman, H.G., "Preliminary Numerical Simulations of a Pulsed Detonation Wave Engine," AIAA Paper 88-2960, July 1988.

[15]Lynch, E.D., and Edelman, R. "Computational Fluid Dynamic Analysis of the Pulse Detonation Engine Concept," AIAA Paper 94-0264, January 1994.

[16]Jachimowski, C.J., "An Analytical Study of the Hydrogen-Air Reaction Mechanism with Application to Scramjet Combustion," NASA Technical Paper 2791, February 1988.

[17]Shapiro, A.H., *The Dynamics and Thermodynamics of Compressible Fluid Flow*, Ronald Press Company, New York, 1953.

[18]Wilson, J., and Paxson, D.E., "On the Exit Boundary Condition for One-dimensional Calculations of Pulsed Detonation Engine Performance," Proceedings of the 18th International Colloquium on Detonation, Explosion, and Reactive Systems, Seattle, WA, July 2001.

[19]Poinsot, T.J., and Lele, S.K., "Boundary Conditions for Direct Simulations of Compressible Viscous Flows," Journal of Computational Physics, Vol. 101, 1992, 104-129.

[20]Gordon S., and McBride, B.J., "Computer Program for Calculation of Complex Chemical Equilibrium Compositions and Applications," NASA Reference Publication 1311, 1994.